



## OPEN

SUBJECT AREAS:  
MASS SPECTROMETRY  
BIOMARKER RESEARCHReceived  
14 October 2014Accepted  
3 February 2015Published  
4 March 2015Correspondence and  
requests for materials  
should be addressed to  
H.G.  
(guhaiwei2004@  
gmail.com)\* These authors  
contributed equally to  
this work.

# Quantitative detection of nitric oxide in exhaled human breath by extractive electrospray ionization mass spectrometry

Susu Pan<sup>1\*</sup>, Yong Tian<sup>2\*</sup>, Ming Li<sup>3</sup>, Jiuyan Zhao<sup>4</sup>, Lanlan Zhu<sup>4</sup>, Wei Zhang<sup>4</sup>, Haiwei Gu<sup>1</sup>, Haidong Wang<sup>1</sup>, Jianbo Shi<sup>2</sup>, Xiang Fang<sup>3</sup>, Penghui Li<sup>1</sup> & Huanwen Chen<sup>1</sup>

<sup>1</sup>Jiangxi Key Laboratory for Mass Spectrometry and Instrumentation, East China Institute of Technology, Nanchang, Jiangxi Province 330013, P. R. China, <sup>2</sup>State Key Laboratory of Environmental Chemistry and Ecotoxicology, Research Center for Eco-Environmental Sciences, Chinese Academy of Sciences, Beijing 100085, P. R. China, <sup>3</sup>National Institute of Metrology, Beijing 100013, P. R. China, <sup>4</sup>Department of Respiratory Medicine, The First Affiliated Hospital of Nanchang University, Nanchang, Jiangxi Province 330006, P. R. China.

**Exhaled nitric oxide (eNO) is a useful biomarker of various physiological conditions, including asthma and other pulmonary diseases. Herein a fast and sensitive analytical method has been developed for the quantitative detection of eNO based on extractive electrospray ionization mass spectrometry (EESI-MS). Exhaled NO molecules selectively reacted with 2-phenyl-4, 4, 5, 5-tetramethylimidazoline-1-oxyl-3-oxide (PTIO) reagent, and eNO concentration was derived based on the EESI-MS response of 1-oxyl-2-phenyl-4, 4, 5, 5-tetramethylimidazoline (PTI) product. The method allowed quantification of eNO below ppb level (~0.02 ppbv) with a relative standard deviation (RSD) of 11.6%. In addition, eNO levels of 20 volunteers were monitored by EESI-MS over the time period of 10 hrs. Long-term eNO response to smoking a cigarette was recorded, and the observed time-dependent profile was discussed. This work extends the application of EESI-MS to small molecules (<30 Da) with low proton affinity and collision-induced dissociation efficiency, which are usually poorly visible by conventional ion trap mass spectrometers. Long-term quantitative profiling of eNO by EESI-MS opens new possibilities for the research of human metabolism and clinical diagnosis.**

Nitric oxide (NO) regulates a great number of biological processes, and its level in living organisms is very sensitive to physiological conditions<sup>1</sup>. Monitoring the concentration of exhaled nitric oxide (eNO) is of substantial interest in metabolism studies and clinical applications, because it is a non-invasive method to characterize airway pathology or pulmonary inflammation for various diseases, such as asthma, chronic obstructive pulmonary disease, lung diseases, etc.<sup>2–10</sup> It also may be useful in identifying lung function deterioration in scleroderma<sup>11</sup>. The level of eNO from Hodgkin disease patients has been found higher than that after remission<sup>12,13</sup>.

To date, several analytical techniques including chemiluminescence<sup>14,15</sup>, electrochemical sensors<sup>15,16</sup>, diamino-fluorescein (DAF-2 and DAF-2DA)<sup>16</sup>, and mass spectrometry<sup>17</sup> have been used for eNO detection. For many years, the method based on measuring chemiluminescence in the photochemical reaction between NO and ozone was considered as the “gold standard” for eNO detection<sup>18</sup>. Reliable quantification of eNO by chemiluminescence is challenging and requires onsite calibration. Significantly different mean eNO values in human beings were reported by the research groups using different instrumentation for chemiluminescence detection<sup>19</sup>. Electrochemical sensing is more direct and simpler for operation, but the selectivity and the detection limit (~5 ppbv) of the currently available NO sensors require further development. Another limitation of electrochemical sensors is their low efficiency in NO multiple flow analysis (various expiratory flow rates for the sampling procedures)<sup>20</sup>. The combination of gas chromatography and mass spectrometry (GC-MS) is a powerful method for the sensitive and reliable detection of eNO in humans<sup>17</sup>. However, the throughput of GC-MS analysis is limited by the necessity of sample preparation, e.g., breath condensation and water removal.



Recently, the possibility of direct human breath analysis was demonstrated using extractive electrospray ionization mass spectrometry (EESI-MS)<sup>21</sup>. In many cases, EESI-MS requires no/minimal sample pretreatment and allows sensitive detection of both volatile and non-volatile compounds in exhaled breath in real time with high throughput. By forming molecular complexes with silver cations ( $\text{Ag}^+$ ), analytes can be detected although they are difficult to be ionized with electrospray ionization (ESI) (e.g.,  $\text{CH}_3\text{-S-CH}_3$ ,  $\text{CH}_3\text{CN}$ , etc.). This substantially enhances the molecular coverage of EESI-MS<sup>22,23</sup>. Improving the specificity of detection is of particular importance for small molecules such as NO, because the tandem MS analysis of NO ions (e.g.,  $\text{NO}^+$ ) cannot be done with commonly used mass spectrometers. However, specific complex formation between NO molecules and  $\text{Ag}^+$  or other metal cations appears to be very difficult. This makes NO and similar compounds in breath and other matrices still invisible to EESI-MS.

In this work, an EESI-MS analytical method has been developed for the quantitative detection of eNO in humans based on the reaction between NO and 2-phenyl-4, 4, 5, 5-tetramethylimidazoline-1-oxyl-3-oxide (PTIO). Detection and quantification of NO has been demonstrated using PTIO as a scavenger molecule<sup>24</sup>. Following a simple chemical mechanism, NO is oxidized by PTIO to yield  $\text{NO}_2$  and 1-oxyl-2-phenyl-4, 4, 5, 5-tetramethylimidazoline (PTI) (Figure 1)<sup>25</sup>. The detection of PTI product can therefore serve to indicate the presence of NO in various samples. In addition, PTIO is also widely used for the quantitative detection of  $\text{NO}^{26}$ . The selectivity for the conversion of PTIO to PTI in NO detection is high<sup>27</sup>, and the reaction of PTIO with NO forms solely PTI and  $\text{NO}_2$ . Although  $\text{NO}_2$  can oxidize PTIO to  $\text{PTIO}^+$ , quantitation of NO based on the yield of PTI is still valid, if an excess of PTIO is provided (this is the case in the current study, and the concentration of NO in breath is generally low)<sup>28</sup>. Usually, breath analysis by EESI-MS is done *in vivo*; i.e., volunteers donate their breath in front of a mass spectrometer in real time. However, the analysis of stationary patients with serious health problems, such as asthma, is difficult using this approach. To make our method more convenient for patients, the breath samples in this study were collected *in situ* by passing exhaled breath through a flow-control unit into collection bottles containing the PTIO solution ( $0.5 \text{ mg L}^{-1}$ ). Following the sample collection, the resulting solution was directly sampled into EESI-MS for the targeted identification of PTI. By measuring the abundance of the characteristic PTI fragment ( $m/z$  144) in the MS/MS detection mode, quantification of eNO content was achieved with a high analysis speed, sensitivity, and specificity. Instead of traditional ESI, EESI, a representative ambient ionization method<sup>29</sup>, was selected as the major detection tool because of its additional advantages of high tolerance to matrix effect and less contamination to the ion source, which helped to collect long-time reproducible and quantitative data.

## Results

**EESI-MS spectra of PTIO.** Because PTIO is a radical molecule, it can produce various by-products during the ionization process. Therefore, EESI-MS analysis of pure PTIO solution provides an important reference/background check before the analysis of reaction products between PTIO and NO. In the EESI-MS spectrum recorded using a

PTIO solution ( $0.5 \text{ mg L}^{-1}$ ), abundant peaks were detected at  $m/z$  203, 219, 234, 235, and 256 (Figure S-1a). The spectrum was dominated by the protonated PTIO ions  $[\text{PTIO}+\text{H}]^+$  ( $m/z$  234), sodiated PTIO  $[\text{PTIO}+\text{Na}]^+$  ( $m/z$  256), and even-electron  $[\text{PTIO}+2\text{H}]^+$  ions ( $m/z$  235). EESI is an ambient ionization technique and NO has already been in the air, which might be the reason why PTI ions ( $m/z$  218 and 219) were produced in Figure S-1a. However, these background signals were subtracted during the following concentration calculations.

In the EESI-MS/MS spectrum of  $[\text{PTIO}+\text{H}]^+$  (Figure S-1b), the major peaks at  $m/z$  114 and  $m/z$  84 were produced due to the cleavage of neutral  $\text{C}_7\text{H}_6\text{NO}$  and  $\text{C}_7\text{H}_6\text{N}_2\text{O}_2$  from the precursor ions to generate  $[\text{C}_6\text{H}_{12}\text{NO}]^+$  ions and  $[\text{C}_6\text{H}_{12}]^+$  ions, respectively. The precursor ions at  $m/z$  234 also lost  $\text{C}_6\text{H}_{10}$  to yield the fragment at  $m/z$  152. In the MS<sup>3</sup> analysis, the product ion at  $m/z$  84 yielded major fragments at  $m/z$  69 and  $m/z$  56 (inset of Figure S-1b). Notably, the experimental parameters such as the ESI voltage, ESI solvent composition, ESI solvent injection rate, sample injection rate, ion-transport capillary temperature, and sheath gas ( $\text{N}_2$ ) pressure were experimentally optimized (detailed in Supplementary Information).

**EESI-MS analysis of PTI formed in the reaction between PTIO and NO gas standard.** The EESI mass spectrum of PTI analyzed from the stock solution ( $0.926 \text{ mg L}^{-1}$ ) was dominated by the protonated PTI ions  $[\text{PTI}+\text{H}]^+$  ( $m/z$  218), while  $[\text{PTI}+2\text{H}]^+$  had a lower intensity ( $m/z$  219) (Figure 2a). MS/MS experiment on the  $[\text{PTI}+\text{H}]^+$  ions generated major fragments at  $m/z$  98, 104, 136, 144, 201, and 203 (Figure 2b). The precursor ions at  $m/z$  218 also lost  $\text{C}_3\text{H}_8\text{NO}$  to yield the fragments at  $m/z$  144 (potential chemical structures are shown in Figure S-2). The MS/MS spectrum of  $[\text{PTI}+2\text{H}]^+$  ( $m/z$  219) (Figure S-3) and its possible fragmentation mechanism (Section 5) are shown in Supplementary Information.

**EESI-MS spectra of PTI after reaction with exhaled NO.** The exhaled breath was passed through the PTIO solution to form PTI product as described in the Experimental section. To exclude the possibility of false-positive MS detection of PTI (Figure S-4a), the MS/MS pattern of  $m/z$  218 ions from breath samples (Figure S-4b) were compared to that from the authentic PTI standard under the same experimental conditions (Figure 2b). The similarity between Figure S-4b and Figure 2b confirmed the successful detection of PTI.

**Calibration curves.** To build calibration curves for PTIO and PTI in our experiments, each standard solution was analyzed 6 times independently under optimized experimental conditions (see Supplementary Information). For PTIO, the MS<sup>2</sup> signal of  $m/z$  84 after background subtraction was plotted as a function of PTIO concentration. The linear response range for PTIO was about 5 orders of magnitude (Figure S-5). The calibration equation was  $\log_{10} I_1$  (intensity of  $m/z$  84, cps) =  $0.7181 \log_{10} C_{\text{PTIO}}$  (concentration,  $\text{ng L}^{-1}$ ) - 0.6131, with a linearity coefficient  $R^2 = 0.995$  using the logarithmic scale. The calibration curve for PTI was built as follows. Standard PTIO solutions were reacted with NO. The concentration of non-reacted PTIO remaining in each solution after the reaction was measured by EESI-MS. By subtracting the final concentration of PTIO from the original PTIO concentration in a standard sample, the amount of PTI product was determined. The PTI product in each reacted standard

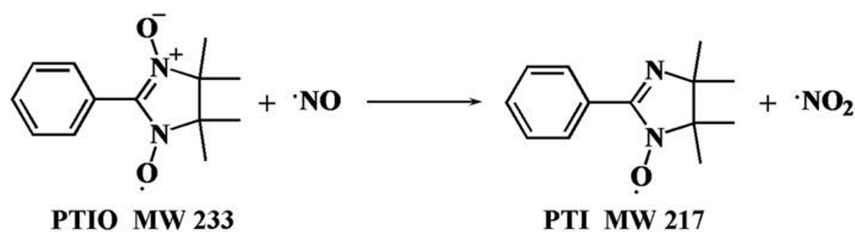


**Figure 1** | The reaction of PTIO with NO.

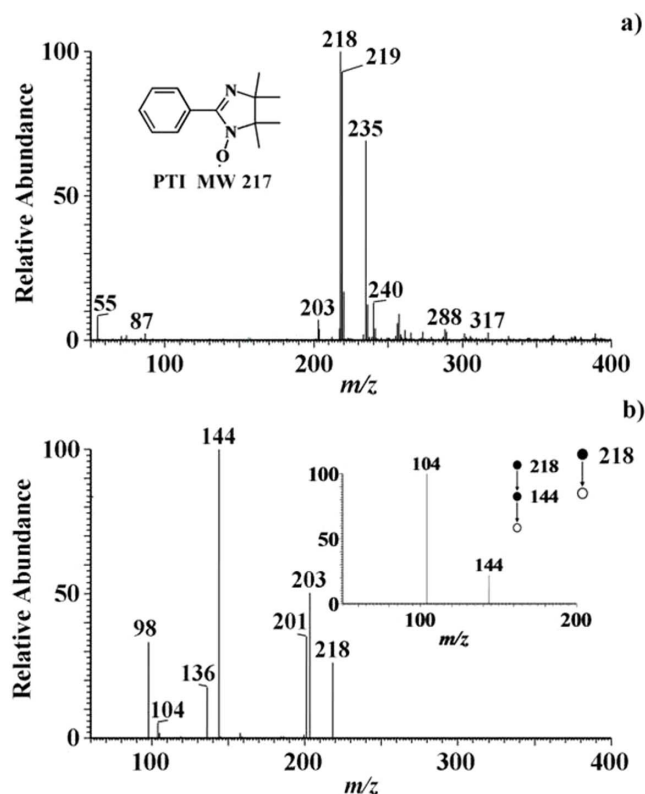


**Figure 2** | EESI-MS spectra of PTI. (a) Full scan EESI-MS mass spectrum of PTI ( $0.926 \text{ mg L}^{-1}$ ); (b) MS<sup>2</sup> spectrum of protonated PTI ( $m/z$  218), and the inset shows the MS<sup>3</sup> spectrum of  $m/z$  218.

solution was then analyzed by EESI-MS. The  $[\text{PTI}+\text{H}]^+$  ion ( $m/z$  218) was selected for MS/MS analysis, and the intensity of  $m/z$  144 fragment was measured.

The calibration for PTI was converted to the calibration for eNO, based on their linear relationship:  $[\text{eNO}] (\text{ppbv}) = 565 [\text{PTI}] (\text{mg L}^{-1})$  (see Supplementary Information). Finally, a calibration curve was obtained for the concentration of eNO depending on the signal intensity of  $m/z$  144. The linear equation in the log/log scale was:  $\log_{10} [m/z$  144, cps] =  $1.0893 \log_{10} [\text{eNO}, \text{ppbv}] + 1.7133$  ( $R^2 = 0.995$ ). The linear region for the calibration curve of eNO spanned 4 orders of magnitude (Figure S-6). The limit of detection (LOD,  $S/N = 3$ ) was determined to be 0.02 ppbv. From six independent measurements the relative standard deviation (RSD) was estimated to be 11.6%.

**Dynamic change of NO level in the exhaled breath from volunteers before and after smoking.** Using the described method, we analyzed the dynamic change of NO observed in breath before and after smoking from 20 volunteers including 12 regular smokers and 8

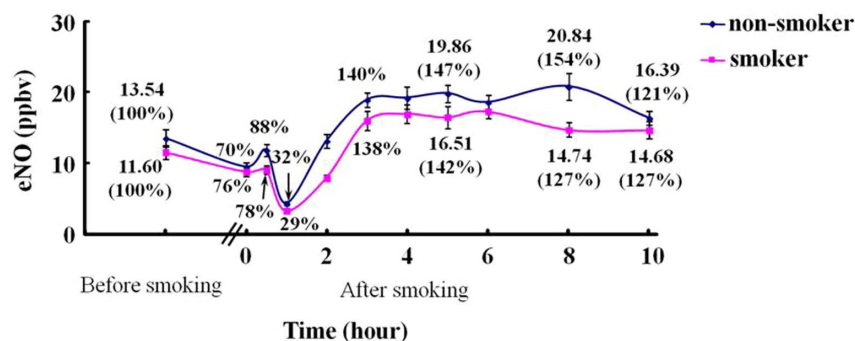


**Figure 3** | Dynamic change of NO levels in the exhaled breath of volunteers before and after smoking one cigarette.

non-smokers. The eNO concentration was plotted as a function of time after smoking a cigarette. Each data point in Figure 3 is the averaged percentage of the eNO concentrations to the first data point (before smoking) on the corresponding dynamic curve (concentration data/the first data on each dynamic curve  $\times 100\%$ ). The recorded 10-h eNO profiles of all the subjects (Figure 3) showed that the mean eNO values of smokers and non-smokers before smoking (the first data points) were 11.6 ppbv and 13.5 ppbv, respectively. NO concentration decreased immediately after smoking down to a mean value of 8.8 ppbv (76%) for smokers and 9.5 ppbv (70%) for non-smokers, and the NO levels increased in about 30 min to 9.1 ppbv (78%) and 11.9 ppbv (88%), respectively. Then the NO concentration further decreased down to the lowest level at 3.3 (29%) ppbv (smokers) and 4.4 (32%) ppbv (non-smokers) in about 1 h. Finally, the NO level increased again in ca. 3 h. Furthermore, we examined the difference between smokers and non-smokers at each time point. It turned out that the most significant difference showed at  $t=8$  hrs with a Student's T-Test P value of 0.000072, and other time points had less difference (e.g.,  $P=0.16$  at  $t=3$  hrs). In addition, we performed the spiking experiment using the breath samples from 5 subjects, which confirmed that our measurements were reliable. As shown in Table S-1, the average recovery rate was 102.6%, with a range of 99.3% to 106.3%.

## Discussion

The observation of abundant  $[\text{PTIO}+2\text{H}]^+$  ions ( $m/z$  235, Figure S-1) in EESI-MS is probably due to the high reactivity of radical PTIO species.  $[\text{PTIO}+2\text{H}]^+$  can be formed by the direct attachment of one  $\text{H}^+$  and one  $\text{H}^+$  to  $\text{PTIO}^{30,31}$ . The MS/MS spectrum of  $[\text{PTIO}+2\text{H}]^+$  ( $m/z$  235) (Figure S-8) and its possible fragmentation mechanism (Section 4) are shown in Supplementary Information. The peaks at  $m/z$  203 and  $m/z$  219 correspond to the species formed via detachment of  $\text{O}_2$  and  $\text{O}$  from PTIO ions, respectively. These species are not observed in the MS/MS spectrum of PTIO ions and are therefore formed in solution rather than by fragmentation.

The fragments at  $m/z$  201, 203, and 98 in the EESI-MS/MS spectrum of PTI product (Figure 2b) are due to the losses of OH,  $\text{CH}_3$ ,  $\text{C}_7\text{H}_6\text{NO}$ , respectively. The product ions at  $m/z$  144 further fragment into  $m/z$  104, probably by the loss of  $\text{C}_3\text{H}_4$  (inset of Figure 2b). The relatively low intensity of PTI signal (compared to the intensity of PTI standard ( $0.926 \text{ mg L}^{-1}$ )) at  $m/z$  218 produced by the reaction of PTIO with breath (Figure S-4a) reflects the usually low concentration of eNO in humans. We excluded the possibility of significant spectral interferences to the detection of PTI because the fragmentation pattern of  $m/z$  218 in breath and reference samples were found to be nearly identical (Figure S-4b and 2b).

The recorded EESI-MS profiles indicate that right after smoking a cigarette the breath NO concentration is initially decreasing (Figure 3). The decrease of eNO within the first few minutes is consistent with the inhibition of nitric oxide synthase (NOS) activity by NO contained in cigarettes<sup>32,33</sup>. The follow-up increase of eNO observed for each individual at about 30 min agrees with the study by Chambers *et al.*<sup>34</sup> The



decrease of eNO signal can be explained by the reduced levels of NOS, the family of enzymes responsible for the NO production<sup>35,36</sup>. Reduced levels of stable end products of NO metabolism (e.g., nitrite and nitrate) have been reported in the saliva and serum of smokers 1 hr after smoking a single cigarette<sup>37</sup>. The oxidant molecules in cigarettes can also contribute to the decrease of NO in breath. Although the exact mechanism why smoking causes long-term fluctuation of eNO remains unclear, the capability of EESI-MS for quantitative detection of eNO makes it a potentially useful platform for more advanced studies of NO metabolism. Notably, the results of spiking experiments further validated that the present method is accurate for the eNO detection from human breath.

To conclude, a novel analytical method has been developed for the rapid and quantitative detection of NO in the exhaled breath with high chemical sensitivity and specificity based on the EESI-MS analysis of PTI produced during the reaction between NO and PTIO. In-situ sample collection makes our method applicable for stationary patients and convenient for large-population studies. The LOD for eNO detection is well below ppb level ( $\sim 0.02$  ppbv), and the relative standard deviation of measured eNO is 11.6%. Using the introduced method, characteristic time profile of eNO was investigated for smoking individuals. The exact mechanism by which smoking induces dynamic changes in the eNO level remains unknown, and the findings reported here offer an alternative analytical tool for advanced studies in this field.

## Methods

**Materials and Reagents.** 2-phenyl-4, 4, 5, 5-tetramethylimidazoleoxyl-1-oxyl-3-oxide (PTIO, >98.0%) was purchased from Tokyo Chemical Industry Co., Ltd. (Tokyo, Japan). The NO gas standard ( $10.2 \times 10^3$  ppbv) was bought from Shenkai Gas Technology Co., Ltd. (Shanghai, China). Methanol (HPLC grade) was bought from ROE Scientific Inc. (Newark, DE, USA). Ultrapure water ( $18.2 \text{ M}\Omega \cdot \text{cm}$ ) was supplied by a Barnstead Nanopure ultrapure water purification system (Thermo Scientific, San Jose, CA, USA). The exhaled breath introduction line was made from the Teflon/polytetrafluoroethylene (PTFE) tube (ID 2 mm, OD 4 mm), which was purchased from Qiwei Industrial Material Co., Ltd. (Dongguan, China). The rotameter used to control the flow rate of exhaled breath was bought from Shenyang Zhengxing Flow Meter Co., Ltd. (Shenyang, China).

**Breath Samples.** The methods were carried out in accordance with the approved guidelines, and all experimental protocols were approved by the Ethics Committee of the East China Institute of Technology and Nanchang University. All the subjects had been informed the content of this experiment before their breath tests, and informed consent was obtained from all subjects. Cigarettes used in the experiments were purchased from a local store. As noted by the manufacturer, a single dosage of cigarette produces 12 mg of tar, 13 mg of carbon monoxide, and 1.2 mg of nicotine. To examine the dynamic change of NO level in the exhaled breath, we collected breath samples from 20 volunteers, including 12 regular smokers and 8 non-smokers, before smoking and after ( $t=0$  hr, 0.5 hrs, 1 hr, 2 hrs, 3 hrs, 4 hrs, 5 hrs, 6 hrs, 8 hrs, 10 hrs). Volunteers for smoking experiments were chosen from healthy adults (age from 20–23). These 20 healthy adult volunteers maintained their normal daily lifestyle during the experiment periods, but were asked to refrain from smoking or exercise at least 6 hours before testing. The zero time point in the recorded PTI profiles corresponded to the moment when a volunteer just finished a cigarette. We also performed Student's T-Test to compare the difference between smokers and non-smokers at each time point. Spiking experiments were performed by bubbling diluted standard NO gas together with breath samples into the PTIO solution. The eNO concentration and the total NO concentration were detected respectively for calculating the recovery rates. Note that the experimental and safety issues have also been addressed according to the local legislation.

**Instrumentation and Working Conditions.** All the experiments were carried out using a homemade EESI source coupled with a Thermo Finnigan hybrid LTQ-XL mass spectrometer (San Jose, CA, USA). The EESI source design and principle were detailed elsewhere<sup>21,22,38</sup>. The LTQ mass analyzer was operated in the positive-ion detection mode, and mass spectra were recorded in the range  $m/z$  50–400. The ESI high voltage was set at +3.0 kV. The temperature of the ion entrance capillary was 300°C. Nitrogen gas (purity  $\geq 99.999\%$ ) was supplied at a pressure of 1.4 MPa. ESI solvent (methanol) and the sample solution were supplied at a flow rate of  $5 \mu\text{L min}^{-1}$  and  $6 \mu\text{L min}^{-1}$ , respectively. The angle between the two spray channels in EESI was 60°. The distance between the sprayer tips was 1.5 mm. The angle between each sprayer and MS inlet capillary was 150°. The distance from the tip of each sprayer to the MS inlet was 5 mm.

In the collision induced dissociation (CID) experiments of PTIO and PTI, the protonated ions at  $m/z$  234 and  $m/z$  218 were selected as the precursor ions,

respectively. The isolation width was 1.2 Da and the collision activation time was 30 ms, with 19–32% (arbitrary units defined by the LTQ instrument) collision energy. The maximum ion injection time was 100 ms and the Automatic Gain Control (AGC) was enabled to regulate the number of ions injected into the ion trap. Other parameters were automatically optimized by the LTQ-MS system.

**Preparation of standard PTIO and PTI solutions.** The stock PTIO solution was prepared by dissolving 10 mg of PTIO into 100 mL of methanol, and then it was stored in the 100-mL brown volumetric flask in the dark. Standard working solutions ( $0.0001$ – $5 \text{ mg L}^{-1}$ ) were prepared by diluting the PTIO stock solution with methanol.

The stock solution of PTI ( $0.926 \text{ mg L}^{-1}$ ) was prepared by reacting 10 mL of PTIO ( $1.0 \text{ mg L}^{-1}$ ) with NO gas ( $10.2 \times 10^3$  ppbv) for about 30 minutes. The stock solution of PTI was diluted serially with methanol to give final dilutions in the range of 1/2.5 to 1/10000  $\text{mg L}^{-1}$ .

**Collection of exhaled NO samples.** 10 mL of standard PTIO solution ( $0.5 \text{ mg L}^{-1}$ ) was added into an empty and dry brown glass reagent bottle. Exhaled NO samples were prepared by bubbling the exhaled breath directly through the PTIO solution ( $0.5 \text{ mg L}^{-1}$ ) via a PTFE tube at a stable exhalation flow rate which was controlled by a rotameter, and the controlled flow rate was  $0.8 \text{ L min}^{-1}$ . Each sample was collected for 150 s (10 successive 15-s samplings). The collected samples were directly analyzed by EESI-MS without further treatment. The experiments were performed at 25°C.

- Murad, F. Discovery of some of the biological effects of nitric oxide and its role in cell signaling (Nobel lecture). *Angew. Chem. Int. Ed.* **38**, 1856–1868 (1999).
- Konvalina, G. & Haick, H. Sensors for breath testing: from nanomaterials to comprehensive disease detection. *Acc. Chem. Res.* **47**, 66–76 (2014).
- Lambert, A. A., Parker, A. M. & Moon, K. K. High-Dose N-Acetylcysteine in Chronic Obstructive Pulmonary Disease, Prone Positioning in Acute Respiratory Distress Syndrome, and Continuous Positive Airway Pressure and Exhaled Nitric Oxide in Obstructive Sleep Apnea. *Am. J. Respir. Crit. Care Med.* **189**, 223–224 (2014).
- Elmasri, M. *et al.* Longitudinal Assessment of High Versus Low Levels of Fractional Exhaled Nitric Oxide Among Children with Asthma and Atopy. *Lung* **192**, 305–312 (2014).
- Paredi, P., Kharitonov, S. A., Meah, S., Barnes, P. J. & Usmani, O. S. A Novel Approach to Partition Central and Peripheral Airway Nitric Oxide. *Chest* **145**, 113–119 (2014).
- Cameli, P. *et al.* Exhaled nitric oxide in interstitial lung diseases. *Respir. Physiol. Neurobiol.* **197**, 46–52 (2014).
- Ricciardolo, F. L. M. Revisiting the role of exhaled nitric oxide in asthma. *Pulm. Med.* **20**, 53–59 (2014).
- De Jongste, J. C., Carraro, S., Hop, W. C. & Baraldi, E. Daily telemonitoring of exhaled nitric oxide and symptoms in the treatment of childhood asthma. *Am. J. Respir. Crit. Care Med.* **179**, 93–97 (2009).
- Dweik, R. A. *et al.* An official ATS clinical practice guideline: interpretation of exhaled nitric oxide levels (FENO) for clinical applications. *Am. J. Respir. Crit. Care Med.* **184**, 602–615 (2011).
- Dummer, J. F. *et al.* Predicting corticosteroid response in chronic obstructive pulmonary disease using exhaled nitric oxide. *Am. J. Respir. Crit. Care Med.* **180**, 846–852 (2009).
- Tiev, K. P. *et al.* Alveolar concentration of nitric oxide predicts pulmonary function deterioration in scleroderma. *Thorax* **67**, 157–163 (2012).
- Guida, G. *et al.* Exhaled nitric oxide and nitric oxide synthase expression in Hodgkin's disease. *Int. J. Immunopathol. Pharmacol.* **22**, 1027–1034 (2009).
- Holmkvist, T., Erlanson, M., Meriläinen, P. & Högman, M. Exhaled nitric oxide is highly increased in a case of Hodgkin's disease. *Acta Oncol.* **42**, 788–789 (2003).
- Kharitonov, S. A. & Barnes, P. J. Clinical aspects of exhaled nitric oxide. *Eur. Respir. J.* **16**, 781–792 (2000).
- Kim, S. H. *et al.* Comparison of two exhaled nitric oxide analyzers: Comparison of two exhaled nitric oxide analyzers: the NIOX MINO hand-held electrochemical analyzer and the NOA280i stationary chemiluminescence analyzer. *Respirology* **17**, 830–834 (2012).
- Planchet, E. & Kaiser, W. M. Nitric oxide (NO) detection by DAF fluorescence and chemiluminescence: a comparison using abiotic and biotic NO sources. *J. Exp. Bot.* **57**, 3043–3055 (2006).
- Leone, A. M. *et al.* Nitric oxide is present in exhaled breath in humans: direct GC-MS confirmation. *Biochem. Biophys. Res. Commun.* **201**, 883–887 (1994).
- American Thoracic Society & European Respiratory Society. ATS/ERS recommendations for standardized procedures for the online and offline measurement of exhaled lower respiratory nitric oxide and nasal nitric oxide. *Am. J. Respir. Crit. Care Med.* **171**, 912–930 (2005).
- Kharitonov, S., Alving, K. & Barnes, P. J. Exhaled and nasal nitric oxide measurements: recommendations. *Eur. Respir. J.* **10**, 1683–1693 (1997).
- Mandon, J. *et al.* Exhaled nitric oxide monitoring by quantum cascade laser: comparison with chemiluminescent and electrochemical sensors. *J. Biomed. Opt.* **17**, 017003 (2012).
- Ding, J. H. *et al.* Development of extractive electrospray ionization ion trap mass spectrometry for *in vivo* breath analysis. *Analyst* **134**, 2040–2050 (2009).
- Chen, H. W., Wortmann, A., Zhang, W. H. & Zenobi, R. Rapid In Vivo Fingerprinting of Nonvolatile Compounds in Breath by Extractive Electrospray



- Ionization Quadrupole Time-of-Flight Mass Spectrometry. *Angew. Chem. Int. Ed.* **46**, 580–583 (2007).
23. Li, M. *et al.* Facilitated Diffusion of Acetonitrile Revealed by Quantitative Breath Analysis Using Extractive Electrospray Ionization Mass Spectrometry. *Sci. Rep.* **3**, 01205 (2013).
  24. Maeda, H., Akaike, T., Yoshida, M. & Suga, M. Multiple functions of nitric oxide in pathophysiology and microbiology: analysis by a new nitric oxide scavenger. *J. Leukocyte Biol.* **56**, 588–592 (1994).
  25. Akaike, T. *et al.* Antagonistic action of imidazolineoxyl N-oxides against endothelium-derived relaxing factor/ bul. NO (nitric oxide) through a radical reaction. *Biochemistry* **32**, 827–832 (1993).
  26. Akaike, T. & Maeda, H. Quantitation of nitric oxide using 2-phenyl-4, 4, 5, 5-tetramethylimidazoline-1-oxyl 3-oxide (PTIO). *Methods Enzymol.* **268**, 211–221 (1996).
  27. Hagos, G. K. *Development of Novel Nitrates for Colon Cancer Chemoprevention* [86] (ProQuest, 2008).
  28. Goldstein, S., Russo, A. & Samuni, A. Reactions of PTIO and Carboxy-PTIO with NO, NO<sub>2</sub>, and O<sub>2</sub><sup>-</sup>. *J. Biol. Chem.* **278**, 50949–50955 (2003).
  29. Takats, Z., Wiseman, J. M., Gologan, B. & Cooks, R. G. Mass spectrometry sampling under ambient conditions with desorption electrospray ionization. *Science* **306**, 471–473 (2004).
  30. Metzger, J. O. & Griep-Raming, J. Electrospray ionization and atmospheric pressure ionization mass spectrometry of stable organic radicals. *Eur. Mass Spectrom.* **5**, 157–163 (1999).
  31. Smith, C. D., Bartley, J. P. & Bottle, S. E. Electrospray mass spectrometry of stable iminyl nitroxide and nitronyl nitroxide free radicals. *J. Mass Spectrom.* **37**, 897–902 (2002).
  32. Assreuy, J., Cunha, F. Q., Liew, F. Y. & Moncada, S. Feedback inhibition of nitric oxide synthase activity by nitric oxide. *Br. J. Pharmacol.* **108**, 833–837 (1993).
  33. Buga, G. M., Griscavage, J. M., Rogers, N. E. & Ignarro, L. J. Negative feedback regulation of endothelial cell function by nitric oxide. *Circ. Res.* **73**, 808–812 (1993).
  34. Chambers, D. C., Tunnicliffe, W. S. & Ayres, J. G. Acute inhalation of cigarette smoke increases lower respiratory tract nitric oxide concentrations. *Thorax* **53**, 677–679 (1998).
  35. Robbins, R. A., Millatmal, T., Lassi, K., Rennard, S. & Daughton, D. Smoking cessation is associated with an increase in exhaled nitric oxide. *Chest* **112**, 313–318 (1997).
  36. Moncada, S. & Higgs, A. The L-arginine-nitric oxide pathway. *N. Engl. J. Med.* **329**, 2002–2012 (1993).
  37. Tsuchiya, M. *et al.* Smoking a single cigarette rapidly reduces combined concentrations of nitrate and nitrite and concentrations of antioxidants in plasma. *Circulation* **105**, 1155–1157 (2002).
  38. Chen, H. W., Venter, A. & Cooks, R. G. Extractive electrospray ionization for direct analysis of undiluted urine, milk and other complex mixtures without sample preparation. *Chem. Commun.* **19**, 2042–2044 (2006).

## Acknowledgments

Authors owe many thanks to Mr. Tengao Zhu, Mr. Tiqiang Zhang, Mr. Lei Hao, and Mr. Jian Chen who helped with recruiting volunteers. This work is jointly supported by the Chinese National Instrumentation Program (No. 2011YQ170067), the National Natural Science Foundation of China (No. 21365001 and 21225522), and China Postdoctoral Science Foundation (No. 2013M530748, 2014T70129).

## Author contributions

S.P., Y.T. and H.G. designed the project, wrote, and revised the manuscript. M.L., X.F., H.W., J.S. and W.Z. gave useful comments and intellectual support, J.Z. and L.Z. performed volunteers' sample detection and data processing, P.L. and H.C. provided important assistance in revising the manuscript. All authors reviewed manuscript.

## Additional information

**Supplementary information** accompanies this paper at <http://www.nature.com/scientificreports>

**Competing financial interests:** The authors declare no competing financial interests.

**How to cite this article:** Pan, S. *et al.* Quantitative detection of nitric oxide in exhaled human breath by extractive electrospray ionization mass spectrometry. *Sci. Rep.* **5**, 8725; DOI:10.1038/srep08725 (2015).



This work is licensed under a Creative Commons Attribution 4.0 International License. The images or other third party material in this article are included in the article's Creative Commons license, unless indicated otherwise in the credit line; if the material is not included under the Creative Commons license, users will need to obtain permission from the license holder in order to reproduce the material. To view a copy of this license, visit <http://creativecommons.org/licenses/by/4.0/>